

PETROGENESIS OF LUNAR METEORITE NORTHWESTERN AFRICA 2977: RARE EARTH ELEMENT GEOCHEMISTRY AND BADDELEYITE Pb/Pb DATING. A. C. Zhang^{1,2}, L. A. Taylor², W. B. Hsu³, C. Floss⁴, X. H. Li⁵, and Y. Liu², ¹Purple Mountain Observatory, Nanjing 210008, China (aczhang@pmo.ac.cn); ²Planetary Geosciences Institute and Department of Earth and Planetary Science, University of Tennessee, Knoxville, TN 37996, USA; ³Faculty of Earth Sciences, China University of Geosciences, Wuhan 430074, China; ⁴Laboratory for Space Sciences and Physics Department, Washington University, Saint Louis, Missouri 63130, USA; ⁵Institute of Geology and Geophysics, Chinese Academy of Sciences, Beijing 100029, China.

Introduction: Northwestern Africa 2977 is an olivine gabbro cumulate lunar meteorite, which is similar to the olivine gabbro portion of lunar breccia NWA 773 [1-3]. However, chronological studies gave various Sm-Nd ages for NWA 773 and NWA 2977 ($\sim 2.865 \pm 0.031$ Ga [4] and 3.10 ± 0.05 Ga [5], respectively). To better understand the petrogenesis of NWA 2977, we performed a detailed petrographic and geochemical study on this meteorite. Here, we report the results of *in situ* REE geochemistry and baddeleyite Pb/Pb dating of NWA 2977.

Analytical methods: REE concentrations in minerals were measured at Washington University, St. Louis with the Cameca IMS-3f ion microprobe following the procedures of [6]. Baddeleyite Pb/Pb dating was carried out by using the Cameca IMS-1280 ion microprobe at the Institute of Geology and Geophysics of Chinese Academy of Sciences, China following the procedures of [7]. Multicollection was used to simultaneously measure secondary ion beam intensities of ^{204}Pb , ^{206}Pb , ^{207}Pb , and $^{90}\text{Zr}_2^{16}\text{O}_2$. The relative yield of each electron multiplier was calibrated using a Phalaborwa baddeleyite standard [8]. Correction for common Pb was made by measuring ^{204}Pb and assuming a common lead composition of $^{206}\text{Pb}/^{204}\text{Pb} = 14 \pm 4$ and $^{207}\text{Pb}/^{206}\text{Pb} = 0.84 \pm 0.2$. Only data with $^{206}\text{Pb}/^{204}\text{Pb} > 1000$ were accepted for the calculation of ages.

Results: REE concentrations in olivine are low and the CI chondrite-normalized pattern is enriched in the HREE, with $\text{Nd} = 0.04 \times \text{CI}$ and $\text{Yb} = 3.6 \times \text{CI}$ (Fig. 1). REE concentrations in pyroxene are related to their occurrences. Low-Ca pyroxene has a CI-normalized HREE-enriched pattern (Fig. 2) with deep negative Eu anomalies. Coarse-grained pigeonite (IP2, IP37, and IP38) has low REE concentrations ($\text{La} 0.3\text{--}1.1 \times \text{CI}$), whereas relatively fine-grained late-stage orthopyroxene (IP8 and IP30) and pigeonite (IP16, IP26, and IP34) have higher REE concentrations ($\text{La} 3.1\text{--}6.6 \times \text{CI}$). Coarse-grained augite (IP1) has a flat HREE pattern, but increasing LREE from La to Sm. Late stage augite (IP20 and IP39) has higher REE concentrations ($\text{La} \sim 14\text{--}16 \times \text{CI}$) and shows increasing LREE concentrations from La ($\sim 14\text{--}16 \times \text{CI}$) to Sm ($\sim 55\text{--}58 \times \text{CI}$), but decreasing HREE concentrations from Gd ($47\text{--}85 \times \text{CI}$) to Lu ($23\text{--}41 \times \text{CI}$). An augite

inclusion in olivine has the highest REE concentrations ($\text{La} 215 \times \text{CI}$) and an essentially flat LREE pattern. All augite grains also show deep negative Eu anomalies.

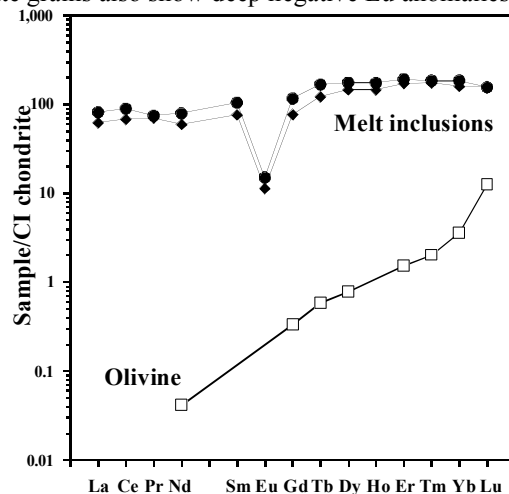


Figure 1. CI chondrite-normalized REE abundances in olivine and melt inclusions.

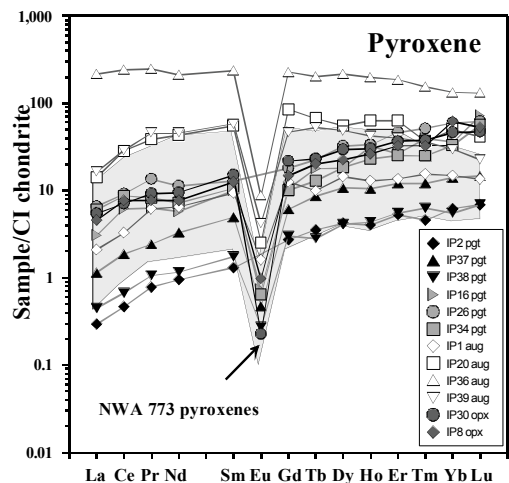


Figure 2. CI chondrite-normalized REE abundances in pyroxene. The shaded area shows data from [9].

Plagioclase has a LREE-enriched pattern with a positive Eu anomaly (Fig. 3). K-feldspar has steeply decreasing LREE from La ($\sim 20\text{--}76 \times \text{CI}$) to Nd ($\sim 1 \times \text{CI}$), a positive Eu anomaly ($\sim 18\text{--}124 \times \text{CI}$) and low HREE abundances that are below detection limits.

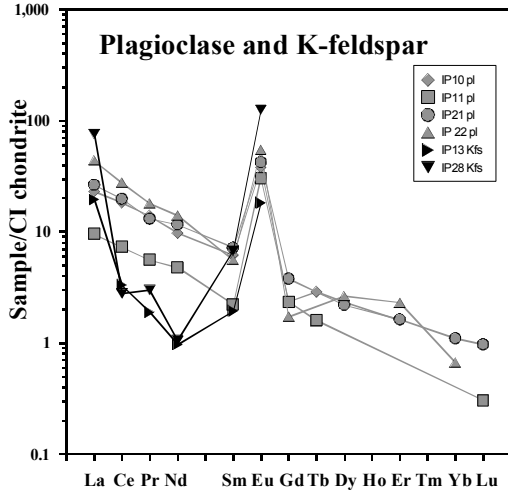


Figure 3. CI chondrite-normalized REE abundance in plagioclase and K-feldspar.

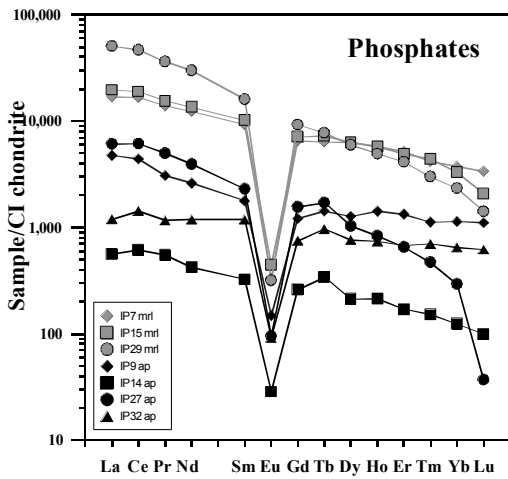


Figure 4. CI chondrite-normalized REE abundances in phosphate minerals.

Merrillite and apatite show LREE-enriched patterns with deep negative Eu anomalies (Fig. 4). Apatite has lower REE concentrations (La $560\text{--}6090 \times \text{CI}$) than merrillite (La $16,865\text{--}50,696 \times \text{CI}$) and shows large variations in REE patterns and abundances. Chlorine-rich apatite (IP9) has higher REE concentrations (La $4754 \times \text{CI}$) than F-rich apatite grains IP14 and IP32 (La $560 \times \text{CI}$ and $1195 \times \text{CI}$, respectively).

Two Si,Al-rich melt inclusions in olivine have almost identical REE concentrations (La $62\text{--}81 \times \text{CI}$) and patterns. HREE concentrations are slightly higher than LREE concentrations and both inclusions show a flat pattern with negative Eu anomalies (Fig. 1).

Ten Pb/Pb measurements on seven baddeleyite grains gave almost identical results within errors (Fig. 5) and yield a weighted mean $^{207}\text{Pb}/^{206}\text{Pb}$ age of 3128 ± 5 (2σ) Ma.

Discussion: The REE abundances and patterns in the NWA 2977 minerals are generally similar to those

in the olivine gabbro portion of NWA 773, which suggests that they could come from a common parent magma. Combined with petrographic and mineralogical information on this meteorite [10], these data show that NWA2977 originated through fractional crystallization. After crystallization of olivine, low-Ca and high-Ca pyroxene, containing relatively low REE concentrations, crystallized almost simultaneously before precipitation of plagioclase. Subsequently, late-stage low-Ca and high-Ca pyroxene, containing high REE concentrations, crystallized together with or after the formation of plagioclase. Finally, phosphate minerals form from the REE-rich residual melt.

Our SIMS baddeleyite Pb/Pb age is in excellent agreement with Sm-Nd and Rb-Sr isochron ages [5], indicating that the crystallization age of NWA 2977 is about 3.1 Ga. The different Sm-Nd ages for NWA 2977 and 773 probably suggest that they have different thermal histories following their crystallization from a common source region.

References: [1] Bunch T. E. et al. (2006) *LPS XXXVII*, Abstract 1375. [2] Burgess R. et al. (2007) *LPS XXXVIII*, Abstract 1603. [3] Zeigler et al. (2007) *LPS XXXVIII*, Abstract 2109. [4] Borg L. E. et al. (2004) *Nature*, 432, 209–211. [5] Nyquist et al. (2009) *MAPS*, 44, A159. [6] Floss C. (2000) *MAPS* 35, 1073–1085. [7] Li X. H. et al. (2009) *G³*, 10, Q04010. [8] Heaman L. M. (2009) *Chemical Geology*, 261, 43–52. [9] Jolliff B. L. et al. (2003) *GCA*, 67, 4857–4879. [10] Zhang A. C. and Hsu W. B. (2008) *MAPS*, 43, A176.

Acknowledgements: The sample was provided by Mr. Michael Farmer. This work was supported by the State Key Laboratory of Lithospheric Evolution at the Institute Geology and Geophysics, Chinese Academy of Sciences, NSFC (Grants 40703015, 40773046), and the Planetary Geosciences Institute at the University of Tennessee, through a NASA Cosmochemistry Program, NNG05GG03G (L.A.T.)

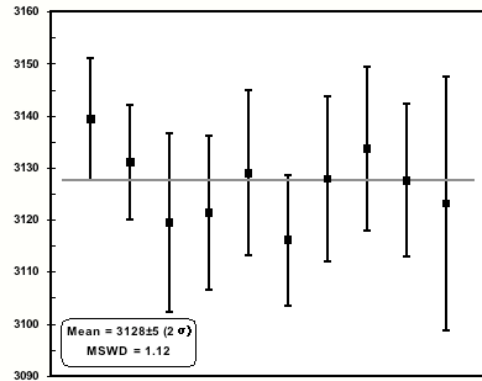


Figure 5. Weighted mean Pb/Pb age of baddeleyite grains in NWA 2977.